Anisotropy of vortex-liquid and vortex-solid phases in single crystals of $Bi_2Sr_2CaCu_2O_{8+\delta}$: Violation of the scaling law

J. Mirković,[1,*] S. E. Savel'ev,[2] E. Sugahara,[1] and K. Kadowaki[1]
[1]*Institute of Materials Science, University of Tsukuba, Tsukuba 305-8573, Japan*
[2]*Frontier Research System, The Institute of Physical and Chemical Research (RIKEN), Wako-shi, Saitama 351-0198, Japan*
(Received 17 June 2002; published 9 October 2002)

The vortex-liquid and vortex-solid phases in single crystals of $Bi_2Sr_2CaCu_2O_{8+\delta}$ placed in tilted magnetic fields are studied by in-plane resistivity measurements using the Corbino geometry to avoid spurious surface-barrier effects. It was found that the anisotropy of the vortex-solid phase increases with temperature and exhibits a maximum at $T\approx 0.97T_c$. In contrast, the anisotropy of the vortex-liquid phase rises monotonically across the whole measured temperature range. The observed behavior is discussed in the context of dimensional crossover and thermal fluctuations of vortices in the strongly layered system.

DOI: 10.1103/PhysRevB.66.132505 PACS number(s): 74.60.Ge, 74.60.Ec, 74.72.Hs

The anisotropic static and dynamical properties of superconductors have commonly been described by the three-dimensional Ginzburg-Landau (3DGL) theory with a single parameter of anisotropy γ defined as a ratio $(m_c/m_{ab})^{1/2}$ of the effective masses m_c and m_{ab} along the *c* axis and in the *a-b* plane, respectively.[1] The anisotropy is related to the basic parameters of a superconductor as $\gamma=\xi_{ab}/\xi_c=\lambda_c/\lambda_{ab}=H_{c2\parallel}/H_{c2\perp}$, where ξ_{ab} and ξ_c are the in-plane and the out-of-plane coherence lengths, λ_c and λ_{ab} are the magnetic-field penetration depths along the *c* axis and in the *a-b* plane, while $H_{c2\perp}$ and $H_{c2\parallel}$ are the out-of-plane and the in-plane upper critical magnetic fields.

Based on 3DGL, Blatter *et al.*[2] obtained the general scaling law, which can be applied for the description of different physical properties of anisotropic superconductors in oblique magnetic fields. For instance, the resistivity in a magnetic field *H*, tilted away from the *c* axis for the angle θ, depends only on the reduced field as

$$\rho(H,\theta)=\rho(H\sqrt{\cos^2\theta+\sin^2\theta/\gamma^2}). \tag{1}$$

The scaling law for the vortex lattice melting magnetic field was derived in a similar manner as

$$H^{melt}(\theta)=H^{melt}(\theta=0)/\sqrt{\cos^2\theta+\sin^2\theta/\gamma^2}. \tag{2}$$

In previous studies it was found that the scaling law describes well experimental data, such as resistivity,[3,4] magnetization,[5] and thermodynamic measurements[6] in $YBa_2Cu_3O_{7-\delta}$ with anisotropy parameter $\gamma\approx 5-7$.[1] Concerning the higher anisotropic layered systems, it was recognized earlier that the dissipation in $Bi_2Sr_2CaCu_2O_{8+\delta}$ depends practically only on the *c*-axis magnetic-field component[7,8] except very close to the *a-b* plane,[9] which is in agreement with the 3DGL scaling law with high anisotropy parameter. However, it was reported[10] that the resistivity data near the *a-b* plane agree better with Thinkam's thin film (hereafter 2DT) model,[11] than with the 3DGL theory. Later, it was also found that the measured anisotropy parameter for $Bi_2Sr_2CaCu_2O_{8+\delta}$ thin films increases with temperature, according to the 2DT model, followed by an indication of the two- to three-dimensional (2D-3D) crossover near the transition temperature T_c.[12,13] On the other hand, recent experimental studies of the first-order vortex-lattice melting transition (VLMT) have shown a linear decay of the out-of-plane melting field with an increasing in-plane magnetic field, even near the *c* axis,[14,15] in a strong contrast to the above-mentioned approaches. In a strict sense, it is reasonable to expect that the scaling law based on the 3DGL model may not be applicable to the extremely anisotropic layered system such as $Bi_2Sr_2CaCu_2O_{8+\delta}$. In this material, the coherence length along the *c* axis at low temperatures is smaller than the lattice parameters of the crystal, which means that the layerness of the material has to be considered.[1] Thus, the 3DGL scaling approach,[2] based on a continuous medium, is not valid due to the discreteness of the system, and therefore, it is not at all trivial that the expressions (1) and (2) are still valid.

Hence, there is still a question of how the anisotropy manifests itself in the different vortex phases in $Bi_2Sr_2CaCu_2O_{8+\delta}$ single crystals. In this paper, we report on the comparative study of the anisotropy of the vortex-solid and vortex-liquid phases in single crystals of $Bi_2Sr_2CaCu_2O_{8+\delta}$. The anisotropy of the first-order vortex-lattice melting transition increases with temperature in the range of $T<0.97T_c$, whereas at higher temperatures, the VLMT anisotropy decreases. In contrast to the anisotropy of the VLMT, the anisotropy of the in-plane resistivity in the vortex-liquid phase increases monotonically with temperature in the whole measured range.

The in-plane resistivity measurements were performed for three as-grown single crystals of $Bi_2Sr_2CaCu_2O_{8+\delta}$ with transition temperatures $T_c^{(I)}=90.3$ K, $T_c^{(II)}=86.0$ K, and $T_c^{(III)}=90.0$ K, for the samples s1, s2, and s3, respectively. In order to probe the true bulk properties, i.e., to avoid the surface-barrier effects that occur in conventional strip geometry,[16] we have used the Corbino electrical contact configuration [see inset in Fig. 1(a)].[17] The diameters of the Corbino discs were $D^{(I)}=1.9$ mm, $D^{(II)}=1.95$ mm, and $D^{(III)}=2.7$ mm while the thickness was $t\approx 20$ μm for all samples. The resistance has been measured by using the ac lock-in technique at a low frequency of 37 Hz. The magnetic field, generated up to 70 kOe by a superconducting split

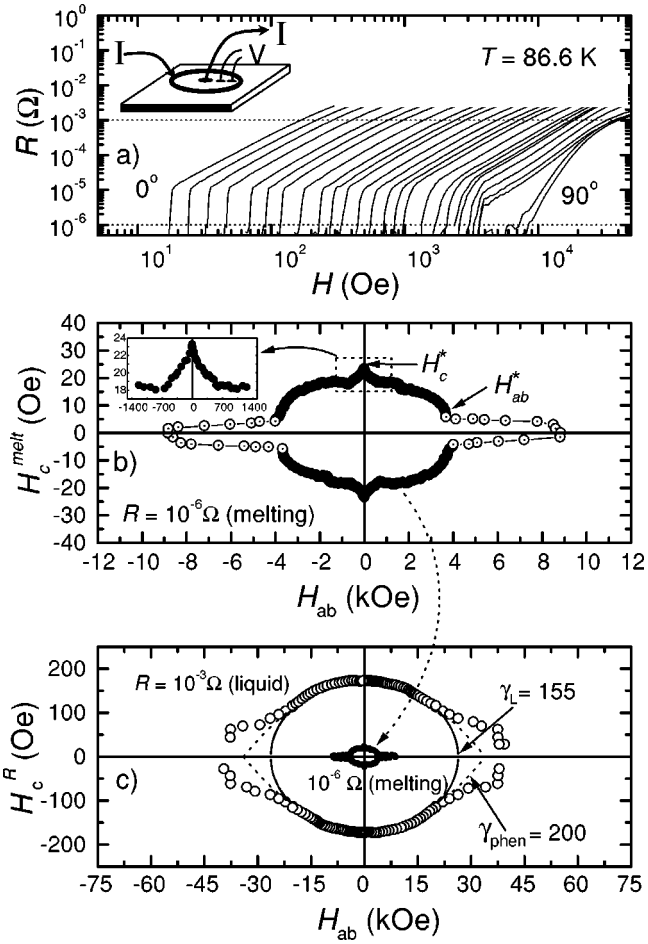

FIG. 1. (a) The magnetic-field dependence of the resistance at various field orientations from $\mathbf{H}\|\mathbf{c}$ (0°) to $\mathbf{H}\|\mathbf{ab}$ (90°) at $T=86.6$ K (sample $s1$). Inset in (a) represents electrical contacts in the Corbino geometry. (b) The H_c-H_{ab} phase diagram of the vortex-lattice melting transition at $T=86.6$ K; the filled symbols mark the first-order phase transition, while the open ones correspond to the continuous resistivity transition. Inset in (b) represents the part of the VLMT phase diagram near the c axis, plotted at a magnified scale. (c) The equiresistance contour at 86.6 K (open symbols) in the vortex-liquid phase. The melting transition from (b) is replotted at the center. The solid line is the ellipse with anisotropy value of $\gamma_L=155$, while the dotted line corresponds to the phenomenological formula wih $\gamma_{phen}=200$.

magnet, was rotated by a fine goniometer with angular resolution of 0.01°, which is better than the mosaicity of the crystals ($\approx 0.03°$).

A typical set of the resistance curves is presented in Fig. 1(a) for $T=86.6$ K. The sharp resistance drop, attributed to the VLMT,[18] is clearly detected across the wide angular range ($\theta<89.86°$).[15] Using the resistance criteria of $R=10^{-6}\ \Omega$, which is set somewhat below the resistivity kink, and $R=10^{-3}\Omega$, which is well above the VLMT anomaly, we construct the phase diagram of the VLMT and the equiresistance contour for the vortex liquid in the H_c-H_{ab} phase plane [Fig. 1(b,c)]. The VLMT phase line $H_c^{\rm melt}(H_{ab})$ [Fig. 1(b)] exhibits the peculiar stepwise shape.[15] Namely, starting from the c axis, the out-of-plane component of the VLMT magnetic field, $H_c^{\rm melt}$, decays linearly with increasing H_{ab},[14] which is associated with the crossing vortex lattice.[19] As the magnetic field further approaches the a-b plane, the linear dependence $H_c^{\rm melt}(H_{ab})$ sharply transforms to the plateau [inset in Fig. 1(b)], which is attributed to the trapping of pancake vortices by Josephson vortices.[20] Very close to the a-b plane ($\theta\approx 89.94°$), the first-order phase transition [filled symbols in Fig. 1(b)] changes to the continuous resistance transition (open symbols),[21] which exhibits the cusp in the H_c-H_{ab} phase plane.[15] In strong contrast to the linear decay of $H_c^{\rm melt}(H_{ab})$ around the c axis, the equiresistance line $H_c^R(H_{ab})$ [Fig. 1(c)] in the vortex-liquid phase demonstrates a smooth quadratic behavior. Near the a-b plane, the equiresistance contour still has a tail, as if it traces the VLMT cusp. The cusplike shape of both the VLMT line and the equiresistance contour, pronounced near the a-b plane, is possibly associated with the intrinsic pinning[22] which, surprisingly, seems to be active even in the vortex-liquid phase, quite far from the VLMT.

We have to mention that our measurements have been done in the H-T region where strong fluctuations are expected. However, according to the theoretical analysis,[23] the fluctuations of the amplitude of the order parameter are relevant only for high magnetic fields $H_c \gtrsim H_{c2\perp}/7 \approx 50(1-T/Tc)$ kOe. Thus, fluctuations in the measured field range are related mostly to the fluctuations of the phase of the order parameter induced by the thermal fluctuations of the positions of vortices, which means that the commonly accepted concept of vortex-solid and vortex-liquid phase is applicable. The next question is how to estimate the anisotropy of the vortex-liquid phase and the VLMT. The smooth quadratic dependence $H_c^R(H_{ab})$, can be derived from the general symmetry law $\rho(H_c,H_{ab})=\rho(H_c,-H_{ab})$, assuming that the resistivity is an analytical function of H_{ab} in the vortex liquid. The last assumption seems to be natural deep in the structureless vortex-liquid phase, where phase transitions are not expected. The simple analysis[24] gives the angular dependence $H_c^R(H_{ab})=H_c^R(0)-H_{ab}^2/[H_c^R(0)\gamma_{phen}^2]$ for the limited angular range of $0°<\theta<90°-57.3°/\gamma_{phen}$, with phenomenological anisotropy parameter $\gamma_{phen}(T,H_c)$. This equation successfully fits our data at 86.6 K in the vortex-liquid phase except very close to the a-b plane with $\gamma_{phen}=200$ [dotted line in Fig. 1(c)]. It is worth noting that the phenomenological angular dependence $H_c^R(H_{ab})$ coincides with the angular dependence of the upper critical field $H_{c2}(\theta)$ for thin superconducting films obtained by Tinkham[11] as $H_{c2}(\theta)\cos\theta/H_{c2\perp}+H_{c2}^2(\theta)\sin^2\theta/\gamma_{2DT}^2H_{c2\perp}^2=1$ with the field independent anisotropy parameter $\gamma_{2DT}\propto 1/\sqrt{1-T/T_c}$. On the other hand, to describe the equiresistance contours in the vortex-liquid phase, it is convenient to apply the more common 3DGL model. Following the 3DGL theory, the $H_c^R(H_{ab})$ line should be an ellipse, $(H_c^R(H_{ab}))^2+H_{ab}^2/\gamma_{3DGL}^2=(H_c^R(0))^2$, with anisotropy γ_{3DGL} being independent of magnetic field and temperature. Fitting the curve in Fig. 1(c) to an ellipse with an anisotropy parameter of 155, we also find a reasonable agreement only in a limited angular range $\theta<89.75°$. Moreover, the empirical anisotropy γ_L of the vortex liquid, obtained by the elliptical fitting of the equire-

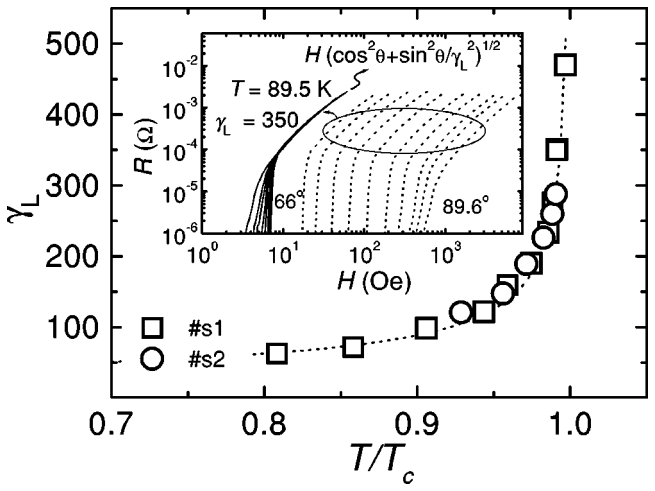

FIG. 2. The temperature dependence of γ_L, extracted by fitting the equiresistance lines to an ellipse, for samples $s1$ and $s2$. The dashed line corresponds to the dependence $\gamma_L = 28/[1-(T/T_c)]^{1/2}$. Inset represents the dotted curves showing the $R(H)$ data obtained at $T = 89.5$ K at various magnetic-field orientations with respect to the c axis (from left, $\theta = 66°$, 74°, 80°, 84°, 86.5°, 88.05°, 88.75°, 89.2°, 89.39°, 89.6°). The solid curves represent scaled resistance curves according to Eq. (1) with $\gamma = \gamma_L = 350$.

sistance contours, increases strongly with temperature in the whole measured temperature interval (Fig. 2), which indicates that the 3DGL scaling law is violated. Thus, the anisotropy parameter γ_L extracted from the ellipse can no longer be attributed to the ratio of the effective masses as assumed in the 3DGL theory, and may reflect the two-dimensional character of the vortex system in analogy to the 2DT approach.[11] Interestingly, the resistivity curves above the VLMT kink, measured at different field orientations ($\theta < 89.6°$, $T = 89.5$ K, $R < 2\times10^{-3}\ \Omega$), collapse into a unique one if the curves $R(H,\theta)$ are scaled in a common way by using Eq. (1) (see inset in Fig. 2) with $\gamma = \gamma_L$. Hence, the anisotropy depends weakly on the resistance level in the vortex liquid but changes sharply around the vortex-lattice melting transition (see Inset in Fig. 2), implying different dimensionality of the probed vortex phases.

Recognizing the fact that the VLMT does not follow the 3D scaling law (2), the effective anisotropy of the VLMT can be estimated by the ratio $\gamma_{melt} = H_{ab}^*/H_c^*$ [for definition of H_c^* and H_{ab}^*, see Fig. 1(b)]. It is necessary to emphasize that the VLMT phase lines, obtained at different temperatures, fall roughly on a unique line if plotted in the phase plane (H_c/H_c^*)-(H_{ab}/H_{ab}^*), as shown in Fig. 3(a). Therefore, the whole VLMT line in the H_c-H_{ab} plane changes proportionally with temperature, which justifies the chosen definition of the anisotropy of the VLMT. The temperature dependences of the characteristic fields H_c^* and H_{ab}^* exhibit different curvatures [see insets in Fig. 3(a)], which result in a maximum of the temperature dependence of the VLMT anisotropy $\gamma_{melt}(T)$ at $T \approx 0.97T_c$, as it is seen in Fig. 3(b). The obtained temperature dependence of γ_{melt} may be approximated by the empirical equation $\gamma_{melt}(T) = \gamma_0(1-T/T_{c1})^{\beta}/(1-T/T_{c2})^{\alpha}$ [the solid line in Fig. 3(b)] with parameters $T_{c1} = 89.4$ K, $T_{c2} = 90.7$ K, $\alpha = 1.08$, and $\beta = 0.6$

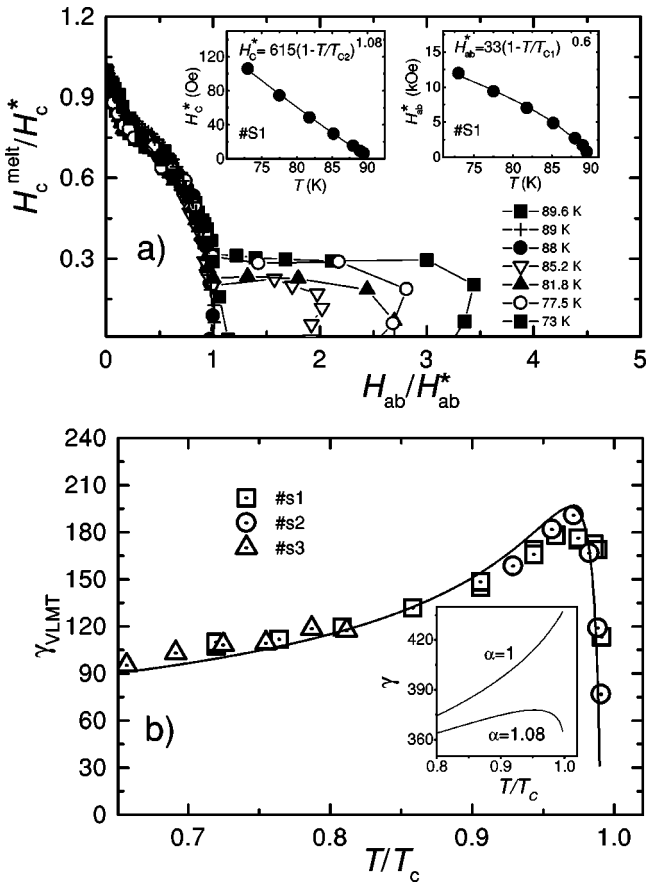

FIG. 3. (a) The phase diagrams of the vortex melting transition plotted in the phase plane (H_c/H_c^*)-(H_{ab}/H_{ab}^*) at different temperatures for $s1$. The left and right insets display the temperature dependence of H_{ab}^* and H_c^*, respectively [for definition of the fields H_{ab}^* and H_c^*, see Fig. 1(b)]. (b) The temperature dependence of the VLMT anisotropy defined as $\gamma_{melt} = H_{ab}^*/H_c^*$, obtained for three samples. The solid line is the empirical equation for $\gamma_{melt}(T)$ discussed in the text. Inset represents the calculated temperature dependence of the anisotropy in the frame of the model (Ref. 26).

obtained by fitting the fields $H_c^*(T) = H_c^*(0)(1-T/T_{c2})^{\alpha}$ and $H_{ab}^*(T) = H_{ab}^*(0)(1-T/T_{c1})^{\beta}$ for the sample $s1$. The two characteristic temperatures (T_{c1}, T_{c2}) in the above empirical formula, may appear due to the fact that the thermodynamic vortex fluctuations have different influence on the interlayer and the intralayer superconductivity in the tilted magnetic fields. The similar maximum of $\gamma(T)$, accompanied by the disappearance of the cusp in the dependence $H_{onset}(\theta)$ ($R(H_{onset}) = 0$) near the a-b plane, was observed earlier in thin films of $Bi_2Sr_2CaCu_2O_{8+\delta}$,[12] although there was neither indication of the VLMT nor clear evidence which vortex phase was probed. The phenomenon[12] was interpreted[13] as a crossover from 2D to 3D behavior, which occurs when the coherence length ξ_c exceeds the distance between CuO_2 layers. In agreement with this scenario, the cusp in the H_c-H_{ab} phase diagram, associated with the continuous resistivity transition, also disappears around the temperature [see Fig. 3(a)] at which $\gamma_{melt}(T)$ is at a maximum.[25] However, based on the 2D-3D crossover, it is impossible to explain why the anisotropy of the vortex-liquid phase still

increases at temperatures $T>0.97T_c$ where $\gamma_{melt}(T)$ decreases. Moreover, the 2D-3D scenario proposed in (Ref. 13) describes only the temperature and angular dependence of the upper critical field $H_{c2}(\theta,T)$, which, strictly speaking, cannot be applied to the VLMT and the equiresistance contours.

Another possible origin of the temperature dependence of the anisotropy could be related to the thermal fluctuations of vortices, which suppresses the Josephson coupling in-between the CuO_2 layers more efficiently than the superconductivity within the layers. As a result, $\lambda_c(T)$ increases faster than $\lambda_{ab}(T)$ and, thus, the anisotropy $\gamma=\lambda_c/\lambda_{ab}$ rises with increasing temperature. According to the model proposed for the magnetic field parallel to the *c* axis,[26] the temperature dependence of the anisotropy is determined by the equation $\gamma^2/\gamma_0^2=\exp(\delta(H_c,T)\gamma^2/\gamma_0^2)$,[27] where $\delta=\pi T H_c s\lambda_{ab}^2(T)\gamma_0^2/2\Phi_0^3$ with $\gamma_0=\gamma(T=0)$. In order to take into account the temperature dependences of the VLMT and equiresistance magnetic fields, the empirical equation $H_c=H_0(1-T/T_c)^{\alpha}$ is used. Since γ is a monotonic function of $\delta\propto T(1-T/T_c)^{\alpha-1}$, the temperature dependence of γ has a maximum approaching T_c, if $\alpha>1$, otherwise γ monotonically increases with *T*. The inset in Fig. 3(b) displays the temperature dependence of γ obtained by using the above equations with $\gamma_0=300$ and $\alpha=1.08$, corresponding to the measured VLMT [inset in Fig. 3(b)], and $\alpha=1$, as assumed for the vortex-liquid phase. Nevertheless, the calculated value of the magnetic field $H_0=29$ kOe disagrees with the experimental value of the *c*-axis field component, but is close to the total applied magnetic field. The discrepancy could be related to the presence of the Josephson vortices that have not been considered in the model.[26] The pancake vortex sublattice interacts with the Josephson vortex sublattice in the crossing lattice structure (set in the tilted magnetic fields) providing the additional mechanism of the renormalization of the anisotropy in the vortex-solid phase.[19,20]

In summary, in contrast to the prevailing belief, we have found clear experimental evidence that neither the 3DGL scaling law nor the 2D Tinkham's model consistently describe the resistivity in the vortex-liquid phase as well as the behavior of the vortex-lattice melting transition, which can qualitatively be accounted for by the thermal fluctuations of vortices.

We thank M. Tachiki, L. N. Bulaevskii, A. E. Koshelev, and V. M. Vinokur for stimulating discussions.

*Present address: Faculty of Sciences, University of Montenegro, P. O. Box 211 81000 Podgorica, Montenegro, Yugoslavia.

[1] G. Blatter *et al.*, Rev. Mod. Phys. **66**, 1125 (1994).
[2] G. Blatter, V.B. Geshkenbein, and A.I. Larkin, Phys. Rev. Lett. **68**, 875 (1992).
[3] Y. Iye *et al.*, Physica C **166**, 62 (1990).
[4] W.K. Kwok *et al.*, Phys. Rev. Lett. **69**, 3370 (1992).
[5] U. Welp *et al.*, Phys. Rev. B **40**, 5263 (1989).
[6] A. Schilling *et al.*, Phys. Rev. B **58**, 11 157 (1998).
[7] P.H. Kes *et al.*, Phys. Rev. Lett. **64**, 1063 (1990).
[8] Y. Iye *et al.*, Physica C **159**, 433 (1989).
[9] H. Raffy *et al.*, Phys. Rev. Lett. **66**, 2515 (1991).
[10] M.J. Naughton *et al.*, Phys. Rev. B **38**, 9280 (1988).
[11] M. Tinkham, Phys. Rev. **129**, 2413 (1963).
[12] E. Silva *et al.*, Phys. Rev. B **55**, 11 115 (1997).
[13] S. Sarti *et al.*, Phys. Rev. B **49**, 556 (1994).
[14] S. Ooi *et al.*, Phys. Rev. Lett. **82**, 4308 (1999).
[15] J. Mirković *et al.*, Phys. Rev. Lett. **86**, 886 (2001).
[16] D.T. Fuchs *et al.*, Nature (London) **391**, 373 (1998).
[17] The radial current distribution results in the circular motion of pancake vortices away from the surface (for Josephson vortices surface barrier is not relevant). Besides, such a current distribution excludes the situation with force-free configuration, since the magnetic field cannot be parallel to the driving current in the whole sample. For more detailed discussion related to the Corbino geometry, see Ref. 15.
[18] S. Watauchi *et al.*, Physica C **259**, 373 (1996).
[19] A.E. Koshelev, Phys. Rev. Lett. **83**, 187 (1999).
[20] S.E. Savel'ev, J. Mirković, and K. Kadowaki, Phys. Rev. B **64**, 094521 (2001).
[21] It is worth noting that the H_c-H_{ab} phase diagram of the VLMT does not practically depend of the resistance criterion if the resistance level is taken below the kink anomaly. On the other hand, the field of the continuous resistance transition varies strongly with the resistance criterion, and a question concerning how the detected resistivity transition is related to the vortex freezing phase transition near the *a*-*b* plane remains still unclear (for more detailed discussion, see Ref. 25).
[22] M. Tachiki and S. Takahashi, Solid State Commun. **70**, 291 (1989).
[23] Z. Tesanović and L. Xing, Phys. Rev. Lett. **67**, 2729 (1991).
[24] In a wide angular range $90°-57.3°/\gamma>\theta$, the equation $R(H_c,H_{ab})=R(H_c,0)+\nu(H_c,T)H_{ab}^2$ with $\nu(H_c,T)=(1/2)(\partial^2R(H_c,H_{ab})/\partial H_{ab}^2)|_{H_{ab}=0}$ can be used, since a linear term does not follow the symmetry restrictions. Thus, $H_c^R(H_{ab})$ should satisfy the equation $R(H_c^R(H_{ab}),0)+\nu H_{ab}^2=R(H_c^R0(0))$, with $R(H_c^R(0))=R^*$ and $R^*=10^{-3}\ \Omega$. The approximate solution of the equation, presented in the text, yields the phenomenological anisotropy $\gamma_{phen}(T,H_c^R(0))=\sqrt{(\partial R(H_c,0)/\partial H_c)|_{H_c=H_c^R(0)}/\nu H_c^R(0)}$.
[25] J. Mirković *et al.*, Physica C **357**, 450 (2001).
[26] L.L. Daemen *et al.*, Phys. Rev. B **47**, 11 291 (1993).
[27] We use the equation obtained in Ref. 26 for the Josephson coupling prevailing over the electromagnetic one, which is valid if $\gamma s\lesssim\lambda_{ab}(T)$. The last condition is satisfied at $T>T^*$, with $T^*/T_c=1-\lambda_{ab}^2(T=0)/\gamma^2s^2=0.8$ for $\lambda_{ab}(T=0)=2000$ Å, $s=15$ Å, and $\gamma=300$.